Neuregulin-1 potentiates agrin-induced acetylcholine receptor clustering through muscle-specific kinase phosphorylation

Shyuan T. Ngo[1], Rebecca N. Cole[3], Nana Sunn[2], William D. Phillips[3,*] and Peter G. Noakes[1,2,*,‡]

[1]School of Biomedical Sciences, University of Queensland, St. Lucia, 4072, Queensland, Australia
[2]Queensland Brain Institute, University of Queensland, St. Lucia, 4072, Queensland, Australia
[3]Physiology and Bosch Institute, The University of Sydney, New South Wales, 2006, Australia

*These authors contributed equally to this work
‡Author for correspondence (p.noakes@uq.edu.au)

Accepted 14 November 2011
Journal of Cell Science 125, 1531–1543

doi: 10.1242/jcs.095109

Summary

At neuromuscular synapses, neural agrin (n-agrin) stabilizes embryonic postsynaptic acetylcholine receptor (AChR) clusters by signalling through the muscle-specific kinase (MuSK) complex. Live imaging of cultured myotubes showed that the formation and disassembly of primitive AChR clusters is a dynamic and reversible process favoured by n-agrin, and possibly other synaptic signals. Neuregulin-1 is a growth factor that can act through muscle ErbB receptor kinases to enhance synaptic gene transcription. Recent studies suggest that neuregulin-1–ErbB signalling can modulate n-agrin-induced AChR clustering independently of its effects on transcription. Here we report that neuregulin-1 increased the size of developing AChR clusters when injected into muscles of embryonic mice. We investigated this phenomenon using cultured myotubes, and found that in the ongoing presence of n-agrin, neuregulin-1 potentiates AChR clustering by increasing the tyrosine phosphorylation of MuSK. This potentiation could be blocked by inhibiting Shp2, a postsynaptic tyrosine phosphatase known to modulate the activity of MuSK. Our results provide new evidence that neuregulin-1 modulates the signaling activity of MuSK and hence might function as a second-order regulator of postsynaptic AChR clustering at the neuromuscular synapse. Thus two classic synaptic signalling systems (neuregulin-1 and n-agrin) converge upon MuSK to regulate postsynaptic differentiation.

Key words: Acetylcholine receptor, Neuromuscular junction, Synaptic plasticity

Introduction

At mature neuromuscular junctions (NMJs), acetylcholine receptors (AChRs) are clustered at high density (~10,000/μm^2) in direct apposition to presynaptic neurotransmitter release sites (Fertuck and Salpeter, 1974; Fertuck and Salpeter, 1976). High density AChR clustering results from: the entrapment of diffuse pre-existing AChRs in the postsynaptic membrane; upregulation of the transcription of AChR subunit genes in the synaptic region and downregulation of the transcription of AChR subunit genes in the extra-synaptic region (Brenner et al., 1990; Merlie and Sanes, 1985; Sanes and Lichtman, 1999). At the NMJ, neural agrin (n-agrin) signals through the muscle-specific kinase (MuSK) by binding its co-receptor, low-density lipoprotein receptor (LDLR)-related protein (LRP4) receptor, to stabilize AChR clusters in the muscle membrane (Ghazanfari et al., 2010; Kim et al., 2008; Valenzuela et al., 1995; Zhang et al., 2008). N-agrin binding to LRP4 enhances LRP4–MuSK interaction leading to autophosphorylation and activation of MuSK (Ghazanfari et al., 2010; Glass et al., 1996; Lin et al., 2008; Zhang et al., 2008). Activation of MuSK triggers positive and negative feedback loops that regulate the phosphorylation (activation) of MuSK, and consequently the degree of AChR clustering. Positive feedback is triggered when MuSK causes the tyrosine phosphorylation of Abl 1/2 and Src-family kinases (Finn et al., 2003; Smith et al., 2001) with Abl kinases acting on MuSK to further increase MuSK phosphorylation and drive AChR clustering (Mittaud et al., 2004). Negative feedback is initiated when MuSK activates Shp2, a tyrosine phosphatase that acts to de-phosphorylate MuSK, resulting in a reduction of AChR clustering (Camilleri et al., 2007; Madhavan and Peng, 2005; Madhavan et al., 2005; Qian et al., 2008; Zhao et al., 2007). Hence, Abl kinases and Shp2 are in a position to regulate n-agrin–MuSK-mediated AChR clustering by modulating the activity of the MuSK receptor.

The developmental and physiological role of neuregulin-1 at the neuromuscular synapse has remained contentious for many years. Neuregulin-1 is a trans-synaptic growth and differentiation factor that signals through ErbB kinase receptors to increase the transcription of synaptic genes such as those for AChRα, AChRε and utrophin (Brenner et al., 1990; Chu et al., 1995; Jo et al., 1995; Martinou et al., 1991; Moscoso et al., 1995; Ngo et al., 2004). However, animals with either nerve-specific knockout of neregulin-1 or muscle-specific knockout of its receptor ErbB2/4 exhibit largely normal adult synapses, throwing into doubt the role of neuregulin-1 in synapse formation (Escher et al., 2005; Fricker et al., 2011; Jaworski and Burden, 2006). Recent muscle culture experiments have reported that neuregulin-1 can either potentiate AChR clustering (Ngo et al., 2004) or de-stabilize

Journal of Cell Science

existing AChR clusters (Trinidad and Cohen, 2004); however, the mechanisms remain unclear and the apparently conflicting results of these two studies have not been resolved. There is evidence that neuregulin-1–ErbB and n-agrin–MuSK signalling pathways might interact. Both pathways can influence postsynaptic gene transcription, and both possess common second messengers (e.g. Cdk5 and Shp2) involved in stabilizing AChR clusters (Fu et al., 2005; Ip et al., 2000; Lacazette et al., 2003; Lin et al., 2005; Qian et al., 2008; Zhao et al., 2007). There is reason to think that n-agrin–MuSK and neuregulin-1–ErbB signalling pathways converge to modulate AChR clustering (Chen et al., 2007; Lin et al., 2005; Ngo et al., 2004; Ngo et al., 2007; Qian et al., 2008; Zhao et al., 2007).

Here we show that, under conditions where n-agrin is limiting, neuregulin-1 potentiated n-agrin-induced AChR cluster formation over a short time frame (4 hours) both in vivo and in vitro. In response to prolonged exposure (12 hours) neuregulin-1 accelerated the disassembly of established n-agrin-induced AChR clusters. The acute potentiation of n-agrin-induced AChR cluster formation involved enhanced MuSK phosphorylation. Neuregulin-1 might serve as a second-order regulator, modulating n-agrin signalling at the synapse during development and in response to physiological challenges.

Results

Exogenous neuregulin-1 increases the size of AChR clusters in vivo

Based on our previous findings that neuregulin-1 can potentiate n-agrin-induced AChR clustering in vitro (Ngo et al., 2004), we sought to determine whether it might do something similar in embryonic muscles. N-agrin, produced by embryonic motor neurons is transported to the nerve terminal where it is essential for stabilizing newly forming postsynaptic AChR clusters (Cohen and Godfrey, 1992; Gautam et al., 1996; Magill-Solc and McMahan, 1988; McMahan, 1990; Reist et al., 1992). Because of the early expression of neuregulin-1 at the developing neuromuscular synapses of both chick and mouse (Loeb et al., 1999; Meyer et al., 1997), we hypothesized that neuregulin-1 might be capable of influencing AChR clustering at this early stage of synapse formation. We investigated the expression of neuregulin-1 receptors in embryonic day (E) 15 mouse sternomastoid muscle, and found that ErbB2 was present over the muscle surface and was coextensive with AChR clusters (Fig. 1A–C, synaptic and extra-synaptic). By contrast, ErbB3 immunostaining appeared to be restricted to the synaptic region, coextensive with AChRs, with a slight shift to the presynaptic side of the AChR cluster (Fig. 1D–F), suggesting that some of the

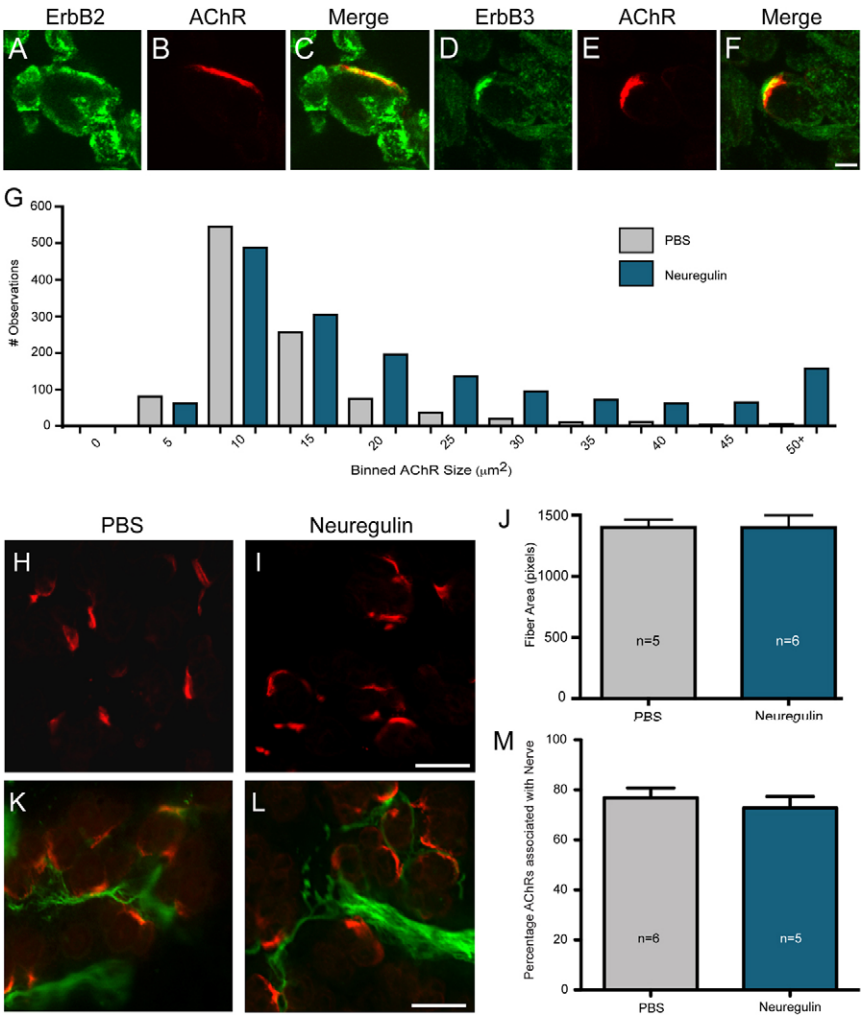

Fig. 1. Exogenous neuregulin-1 increases the size of AChR clusters in vivo. (**A**–**C**) Immunofluorescence staining in E15 sternomastoid muscle reveals ErbB2 to be present over the muscle surface and co-extensive with AChRs. (**D**–**F**) ErbB3 expression is restricted to AChR-rich regions with a slight shift to the pre-synaptic side of AChR cluster (F), suggesting that some of the ErbB staining is presynaptic. Scale bar: 20 μm. (**G**) The sternomastoid muscles of E15 mouse embryos were injected in utero with recombinant neuregulin-1 protein (33 nM). AChR cluster size was quantified 4 hours post injection. The frequency histogram summarizes the number of observations per binned AChR size between PBS- and neuregulin-1-injected embryos. Exogenous neuregulin-1 protein significantly increased AChR cluster size when compared with PBS-injected controls ($P<0.0001$, 1183 AChR clusters for PBS injections across five embryos and 1826 AChR clusters for neuregulin-1 injections across five embryos; Mann–Whitney *U*-test). (**H**,**I**) Sample images of AChR clusters in a control PBS–injected embryo (H) and neuregulin-1 injected embryo (I). (**J**) Muscle cross-sectional area of PBS- and neuregulin-1-injected muscles. Values are means ± s.e.m. Injection of neuregulin-1 did not change the cross-sectional area of muscle fibres. (**K**,**L**) Sample images from PBS-injected (K) and neuregulin-1-injected (L) muscles re-stained for the presence of AChRs (Alexa-Fluor-555–α-BTX, red) and motor nerve endings (anti-neurofilament and anti-synaptophysin cocktail, green). (**M**) Quantification of the percentage of AChR clusters associated with motor nerve endings (means ± s.e.m.; $P=0.5115$, $n=6$ PBS-injected embryos and $n=5$ neuregulin-injected embryos, unpaired *t*-test). Scale bars: 50 μm (H–L).

ErbB3 is presynaptic. Subsequently, using ultrasound biomicroscopy, sternomastoid muscles of mouse embryos were injected with either phosphate-buffered saline (PBS; Fig. 1H) or recombinant neuregulin-1 protein (33 nM) combined with Fluoresbrite® Yellow Green Microspheres (Fig. 1I) during this period of synapse formation (E15) (Lupa and Hall, 1989; Noakes et al., 1993). We examined a 100 μm region surrounding the injection site (identified by fluorescent beads, not shown). Four hours after the injection there was a significant increase in the mean area of AChR clusters in neuregulin-1-injected muscles compared with PBS-injected controls [12.33 μm^2 with PBS and 30.80 μm^2 (mean values) with neuregulin-1; $P<0.0001$, 1183 AChR clusters for PBS injections across five embryos ($n=5$) and 1826 AChR clusters for neuregulin-1 injections across 5 embryos ($n=5$); Mann–Whitney *U*-test; Fig. 1G]. This increase in AChR cluster area was not a result of muscle hypertrophy as there was no increase in the cross-sectional area of muscle cells (Fig. 1J). There was no significant change in the proportion of AChR clusters associated with nerve staining [i.e. AChRs that were ≤5 μm away from neurofilament-synaptophysin-stained nerves (Fig. 1K–M), $P=0.5115$, $n=6$ embryos for PBS and $n=5$ embryos for neuregulin-1, unpaired *t*-test]. Nor was there any increase in the total number of AChR clusters between PBS-injected and neuregulin-1-injected embryos ($P=0.0614$, $n=5$ embryos per group, unpaired *t*-test). Hence, neuregulin-1 would appear to enhance the growth of pre-existing synaptic AChR clusters in these developing muscles (Fig. 1G).

Life-cycle of AChR cluster formation and disassembly

When n-agrin is added to cultured myotubes the number of AChR clusters first rises, reaching a peak after 4 hours, then declines at later time points (Ferns et al., 1996; Ngo et al., 2004). To gain a clearer idea of the dynamics of AChR clustering, we used the C2C12 myoblast cell line and time-lapse imaging to follow the life cycle of the largest AChR cluster that formed on each of nine myotubes over 12 hours of n-agrin treatment. AChR clusters were defined as discrete, uninterrupted areas of intense α-bungarotoxin fluorescence, typically extending along the long axis of the myotube. Images were taken at 10-minute intervals (Fig. 2A). At 4 hours, six large clusters were fully assembled (Fig. 2A). Cluster number one arose from the coalescence of smaller AChR clusters between 40 and 210 minutes after the

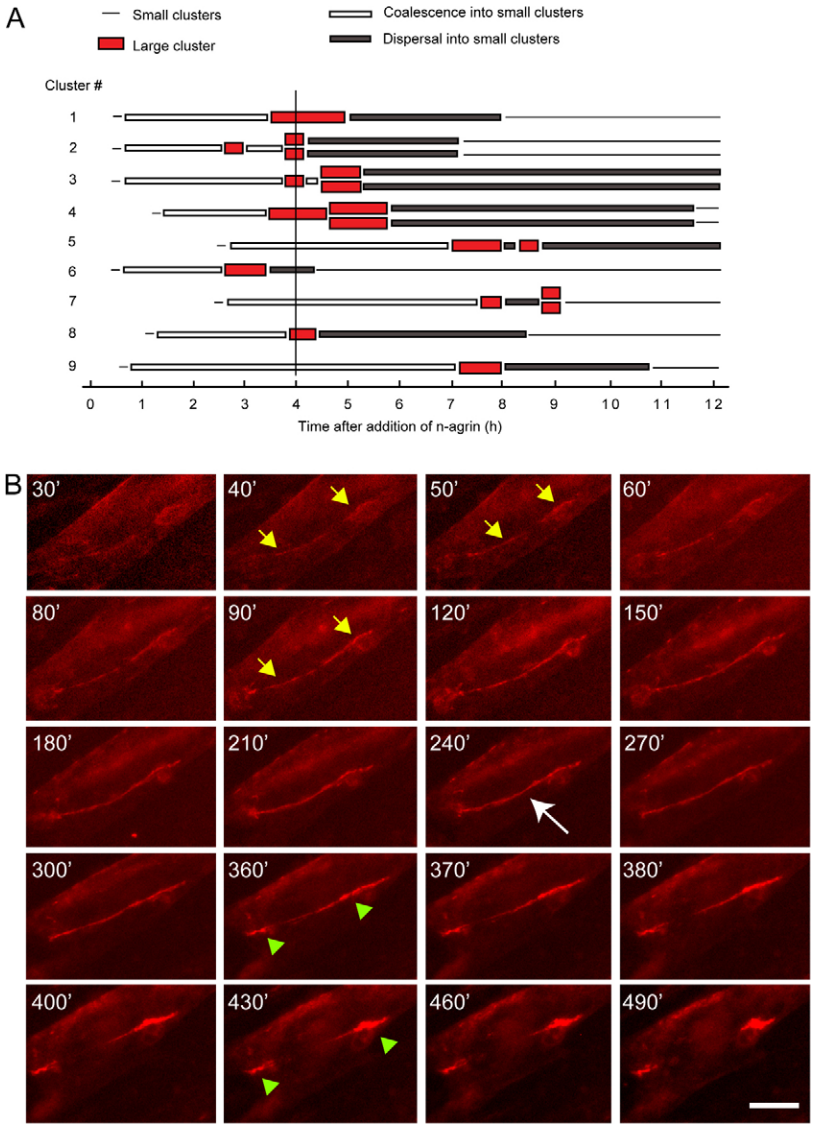

Fig. 2. N-agrin causes time-dependent AChR clustering and disassembly. Time-lapse studies were conducted on C2C12 myotubes treated with 10 nM n-agrin for 12 hours. AChRs were considered to be a large AChR cluster when they were ≥25 μm in their longest dimension (i.e. uninterrupted staining of the longest dimension in the cluster ≥25 μm). (**A**) Time-lines summarizing the formation and dispersal of nine large AChR clusters during prolonged treatment with n-agrin. AChR clusters formed from the coalescence of small AChR clusters and survived 49±11 minutes before breaking up into smaller AChR clusters. Sometimes the established large AChR cluster (red rectangle) transiently split into two large AChR clusters (cluster 4) or smaller AChR clusters before reassembly of the smaller fragment AChR clusters into a single large AChR cluster (cluster 5) or two large clusters (clusters 2, 3 and 7). (**B**) Time-lapse images showing the formation of a large AChR cluster (cluster 1 in A; white large arrow) from small AChR clusters (yellow arrows) and the subsequent dispersal into small AChRs (green arrowheads) between 30 and 490 minutes. Scale bar: 25 μm. Time in minutes is given in each panel. The vertical line through the 4-hour time point in A, indicates that at 4 hours, six out of the nine AChR clusters were classified as large clusters.

addition of n-agrin (Fig. 2A,B). The resultant large cluster remained intact for approximately 1.5 hours before progressively breaking up into smaller clusters over the subsequent 3 hours. The life-cycles of large AChR clusters fell into three stages (summarized in Fig. 2A): (1) the formation of small AChR clusters; (2) coalescence of a group of such small AChR clusters into a large AChR cluster; and (3) subsequent fragmentation of the large cluster into smaller AChR clusters. In each instance the formation of large AChR clusters resulted from the coalescence of small AChR clusters in the immediate vicinity of where the large AChR cluster would subsequently form. A large contiguous AChR cluster (largest clusters ranging from 41 to 273 μm^2) arose from the aggregation of several smaller AChR clusters (Fig. 2B, 30–210 minutes). The formation of each large AChR cluster occurred approximately 2–6 hours after the appearance of small AChR clusters.

Of the nine large AChR clusters tracked, none survived intact for more than 90 minutes before breaking up into smaller AChR clusters. In five of the nine cases, the break-up of the large single AChR cluster was followed by the formation of two large AChR clusters (cluster 4) or a transient partial or complete reassembly of the smaller fragment AChR clusters into a single large AChR cluster (cluster 5) or two large clusters (cluster numbers 2, 3 and 7), prior to final disassembly (Fig. 2A). By the end of the 12-hour imaging period, all but three of the large clusters had broken down into small clusters, or had completely dispersed (Fig. 2A). Thus, in C2C12 myotubes at least, n-agrin instigates a process that involves an initial formation of small AChR clusters, these then coalesce to form a larger AChR cluster that subsequently breaks up into smaller AChR clusters (Fig. 2). Factors that influence the number and size of large n-agrin-induced AChR clusters might then act at any or all of these transition points in the life cycle of the primitive AChR cluster. Notably there was a time-dependent shift, occurring roughly 4 hours after the addition of n-agrin, from an initial tendency of AChR cluster assembly, toward disassembly. This is in line with previous studies that have quantified the number of large n-agrin-induced AChR clusters at this time-point (Ferns et al., 1996; Ngo et al., 2004). Thus agents that act acutely to enhance assembly of AChR clusters could have different effects when applied for prolonged periods.

Neuregulin-1 modulates AChR cluster formation and disassembly

Our previous work showed that neuregulin-1 could potentiate n-agrin-induced AChR clustering in C2C12 myotubes (Ngo et al., 2004), whereas others have reported that neuregulin-1 disassembled C2C12 AChR clusters over a longer time frame (Trinidad and Cohen, 2004). To address this apparent contradiction, we repeated our experiments and compared short and long treatment periods. We used a concentration of n-agrin that produced half-maximal AChR clustering (1 nM) in combination with a concentration of neuregulin-1 (3 nM) sufficient to induce AChRε subunit gene (*Chrne*) transcription (Ngo et al., 2004). In the continued presence of n-agrin, addition of neuregulin-1 over a 4-hour treatment period produced a 1.6-fold increase in the number of large AChR clusters (≥25 μm in length) per myotube segment compared with myotubes treated with half-maximal n-agrin alone (Fig. 3A). The same treatments applied for 12 hours produced very different results. Myotubes treated with 1 nM n-agrin for 12 hours retained only one third the number of large (≥25 μm) AChR clusters present after 4 hours of treatment (Fig. 3A,B). This is consistent with the observation that the number of large AChR clusters peaked at approximately 4 hours of n-agrin treatment and subsequently declined (Fig. 2) (Ngo et al., 2004). These results extend our observations that there is a time-dependent loss of large AChR clusters in cultures continually exposed to n-agrin. Importantly, the observed loss of large AChR clusters from myotubes was greater (2.4-fold) when neuregulin-1 (3 nM) was added in the ongoing presence of n-agrin (Fig. 3B). These results suggest that neuregulin-1 can augment the n-agrin-induced formation of AChR clusters (a rapid

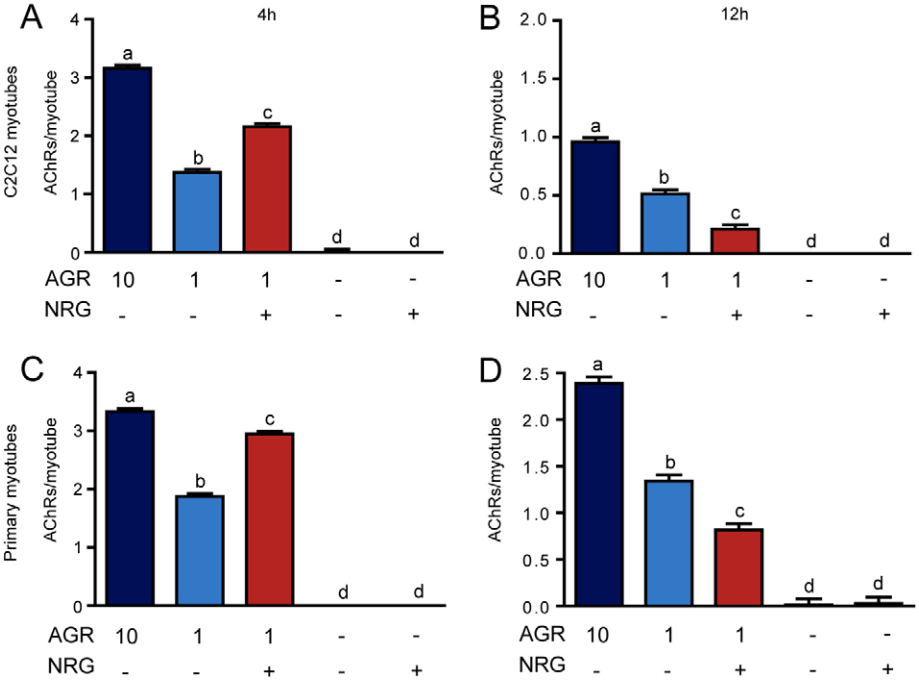

Fig. 3. Neuregulin-1 modulates n-agrin-induced AChR clustering. The formation and dispersal of large AChR clusters (≥25 μm) was analyzed in mouse myotubes treated with continuous n-agrin (AGR) plus or minus neuregulin-1 (NRG) for either 4 or 12 hours. (**A**) In C2C12 myotubes, neuregulin-1 potentiated the number of AChR clusters formed over 4 hours in response to a sub-maximal concentration (1 nM) of n-agrin (bars 2 and 3, $P<0.0001$, $n=3$, ANOVA). (**B**) In C2C12 cultures, neuregulin-1 exacerbated the loss of AChR clusters over 12 hours when compared with n-agrin treatment alone (bars 2 and 3, $P<0.0001$, $n=3$, ANOVA). (**C**) In primary myotubes, neuregulin-1 again caused a strong potentiation of n-agrin-induced (1 nM) AChR clustering in the first 4 hours of exposure (bars 2 and 3, $P<0.005$, $n=3$, ANOVA). (**D**) In primary myotubes exposed to n-agrin for 12 hours, neuregulin-1 exacerbated the loss of AChR clusters (bars 2 and 3, $P<0.0005$, $n=3$, ANOVA). 1 and 10=1 nM and 10 nM respectively. Different lowercase letters indicate significant differences between groups. Values are means ± s.e.m.

event) but also accelerate AChR cluster disassembly when applied for a longer time.

Because C2C12 cells are an immortalized cell line, experiments were repeated in primary mouse muscle cultures. Primary myotubes treated with 1 nM n-agrin and 3 nM neuregulin-1 for 4 hours exhibited a significant ($P<0.005$) increase in the number of large (≥25 μm) AChR clusters compared with half-maximal n-agrin treatment alone (Fig. 3C). Over 12 hours, and in the continued presence of n-agrin, 3 nM neuregulin-1 also caused a significantly greater ($P<0.0005$) loss of large AChR clusters than half-maximal n-agrin treatment alone (Fig. 3D). These results were similar to what we observed in C2C12 cultures (Fig. 3A,B), although large AChR clusters on primary myotubes appeared somewhat more stable over the 12-hour treatment period than those on C2C12 myotubes (compare Fig. 3B with 3D). These results in primary cultures confirm the ability of neuregulin-1 to potentiate n-agrin-induced AChR clustering and to exacerbate AChR cluster loss over longer treatment times.

Neuregulin-1 potentiates n-agrin-induced AChR clustering through ErbB2

In order to determine whether neuregulin-1 potentiation of n-agrin-induced AChR clustering occurred through a neregulin-1–ErbB receptor interaction, we first identified the expression of ErbB receptors on C2C12 myotubes. Previous studies showed that ErbB2 receptors are expressed in C2C12 myotubes (Jo et al., 1995). Using immunofluorescence, we identified ErbB2 adjacent to or within the vicinity of n-agrin-induced AChR clusters (Fig. 4A). Given the proximity of ErbB2 to AChRs, we next examined whether neuregulin-1 acts through ErbB2 to potentiate n-agrin-induced AChR clustering. To address this, we used the ErbB2 inhibitor PD168393 (Calvo et al., 2011). C2C12 myotubes were cultured with 1 nM n-agrin in the presence or absence of 3 nM neuregulin-1, and each of these were tested in the presence or absence of 10 μM PD168393 (Fig. 4B). Treatment with PD168393 alone for 4 hours produced no AChR clusters (Fig. 4B, bar 6). In the presence of 1 nM n-agrin, PD168393 did not alter the number of AChR clusters compared with n-agrin treatment alone (Fig. 4B, bars 1 and 3). As previously shown, treatment of myotubes with 1 nM n-agrin and 3 nM neuregulin-1 led to an increase in the number of large AChR clusters compared with n-agrin treatment alone (Fig. 4B, bars 1 and 2). In the presence of PD168393, however, neuregulin-1 was no longer able to induce a significant increase in the number of large n-agrin-induced AChR clusters (Fig. 4B, bars 2 and 4). Hence, neuregulin-1 potentiates n-agrin-induced AChR clustering through the ErbB2 receptor.

Neuregulin-1 can act only in unison with n-agrin

Soluble isoforms of neuregulin-1 become concentrated at developing synapses by their interaction with heparan sulphate proteoglycans (HSPGs) (Loeb et al., 1999). Given that n-agrin is a HSPG, we next examined whether the n-agrin-induced AChR clustering potentiated by neuregulin-1 required the concurrent presence of n-agrin. Previous work showed that a brief (5 minutes) exposure to n-agrin was sufficient to induce maximal AChR clustering (Mittaud et al., 2004). We tested the effect of pulsed exposure of myotubes to 1 nM n-agrin on the number of large (≥25 μm) AChR clusters 4 hours after the pulse treatment. In agreement with Mittaud et al. a 5-minute n-agrin

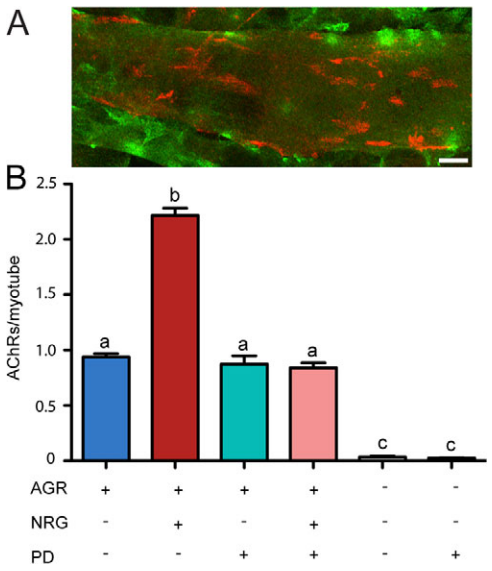

Fig. 4. Neuregulin-1 potentiates n-agrin-induced AChR clustering through ErbB2. (**A**) ErbB2 receptor immunostaining (green) and AChR clusters (red) are coexpressed on the surface of C2C12 myotubes after 4 hours n-agrin treatment. Scale bar: 20 μm. (**B**) A 4-hour treatment of myotubes with n-agrin (AGR, 1 nM) plus neuregulin-1 (NRG, 3 nM) led to a significant potentiation in AChR cluster number compared with n-agrin treatment alone (bars 1 and 2, $P<0.0001$, $n=3$, ANOVA). In the presence of the ErbB2 inhibitor, PD168393 (PD, 10 μM), neuregulin-1 was no longer able to potentiate n-agrin-induced AChR clustering (compare bar 2 with bar 4; $P<0.0001$, $n=3$, ANOVA). Different lowercase letters indicate significant differences between groups at $P<0.0001$. Bars with the same superscript are not significantly different. Values are means ± s.e.m.

pulse treatment of C2C12 myotubes led to significant ($P<0.01$) subsequent AChR cluster formation (Mittaud et al., 2004). However, we found that a single 5-minute or 10-minute pulse of 1 nM n-agrin produced significantly fewer large AChR clusters than continual exposure to 1 nM n-agrin over the full 4-hour period (Fig. 5A).When the 5-minute treatment with 1 nM n-agrin was replaced with 3 nM neuregulin-1 for the remaining 4 hours, there was no change in the number of large AChR clusters compared with myotubes treated with n-agrin alone for 5 minutes (Fig. 5B). Neuregulin-1 only potentiated n-agrin-induced AChR cluster formation when myotubes were concurrently exposed to neuregulin-1 and n-agrin.

Expression levels of synaptic mRNA transcripts

Neuregulin-1 has previously been shown to induce AChR subunit gene transcription in muscle cells (Brenner et al., 1990; Chu et al., 1995; Martinou et al., 1991; Ngo et al., 2004). It has been suggested that n-agrin can also influence AChR and MuSK gene expression. We therefore examined the possibility that neuregulin-1 might potentiate n-agrin-induced AChR clustering indirectly, by increasing the expression of mRNAs encoding AChRα subunit and MuSK. C2C12 myotubes were treated for 4 hours with n-agrin (1 nM) in the presence or absence of neuregulin-1 (3 nM) and mRNA levels were then analyzed. Over 4 hours, none of the treatments produced any significant change in the levels of AChR and MuSK mRNA transcripts relative to untreated controls (supplementary material Fig. S1). These findings suggest that neuregulin-1 potentiates n-agrin-induced

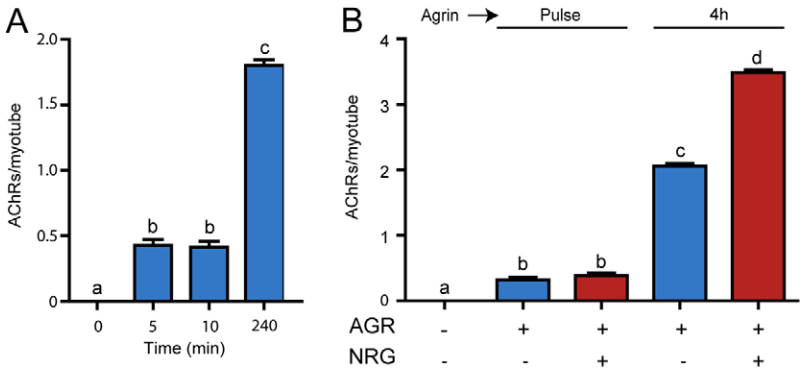

Fig. 5. The potentiation of AChR clustering by neuregulin-1 requires n-agrin. (**A**) Pulse treatment of C2C12 myotubes with 1 nM n-agrin for 5 or 10 minutes induced significant numbers of large AChR clusters (≥25 μm, $P<0.01$, $n=3$, ANOVA) when counted 4 hours later. Treatment with 1 nM n-agrin for 4 hours resulted in higher numbers of AChR clusters ($P<0.01$, $n=3$, ANOVA). (**B**) When pulse treatment with 1 nM n-agrin (AGR) for 5 minutes was followed by a 4-hour treatment with neuregulin-1 (NRG, 3 nM, in the absence of n-agrin), no potentiation was found in the number of large AChR clusters (≥25 μm, compare bars 2 and 3). Thus, neuregulin-1 was able to increase the number of n-agrin-induced AChR clusters (≥25 μm) only when myotubes were exposed concurrently to n-agrin (1 nM; $P<0.005$, $n=3$, ANOVA). Different lowercase letters indicate significant differences between groups. Values are means ± s.e.m.

AChR clustering in a manner that is independent of transcription. Our results do not exclude the longer-term effects of neuregulin-1 reported by others (after overnight treatment) or the effects of n-agrin in cultures of avian muscle (Brenner et al., 1990; Chu et al., 1995; Lacazette et al., 2003; Li and Loeb, 2001; Martinou et al., 1991; Ngo et al., 2004).

Neuregulin-1 potentiation of AChR clustering does not depend upon calpain or cyclin-dependent kinase 5

Calpain and Cdk5 are involved in a partially defined pathway of AChR cluster disassembly (Chen et al., 2007; Lin et al., 2005). Calpain functions upstream of Cdk5 in the acetylcholine-induced disassembly of AChR clusters (Chen et al., 2007). We therefore wanted to determine whether neuregulin-1 impinged upon this pathway. To address this, we first used the calpain inhibitor, calpeptin (Tsujinaka et al., 1988). C2C12 myotubes were cultured with 1 nM n-agrin in the presence or absence of 3 nM neuregulin-1, and each of these were tested in the presence or absence of 20 μM calpeptin (Fig. 6A). Treatment with calpeptin alone for 4 hours produced no AChR clusters (Fig. 6A, bar 6), but in the presence of 1 nM n-agrin, calpeptin increased the number of AChR clusters compared with the number obtained with 1 nM n-agrin alone (Fig. 6A, bars 1 and 3). Nevertheless, in the presence of calpeptin, neuregulin-1 still produced a significant ($P<0.001$) further potentiation of n-agrin-induced AChR clustering (Fig. 6A, bars 3 and 4).

Next we used the Cdk5 inhibitor, roscovitine (2 μM), to investigate the involvement of Cdk5 (Meijer et al., 1997). C2C12 myotubes were treated for 4 hours with 1 nM n-agrin with or without 3 nM neuregulin-1 in the presence or absence of roscovitine. Over this 4-hour period, roscovitine did not alter the number of large AChR clusters (≥25 μm) induced by n-agrin (Fig. 6B, bars 1and 3), nor did roscovitine affect the potentiation of AChR clustering by neuregulin-1 (Fig. 6B, bars 2 and 4). These results suggest that neuregulin-1 potentiation of n-agrin-induced AChR clustering is independent of the calpain–Cdk5 pathway described previously.

Neuregulin-1 potentiates tyrosine phosphorylation of MuSK

N-agrin-induced AChR clustering requires tyrosine phosphorylation of MuSK (Herbst and Burden, 2000). We

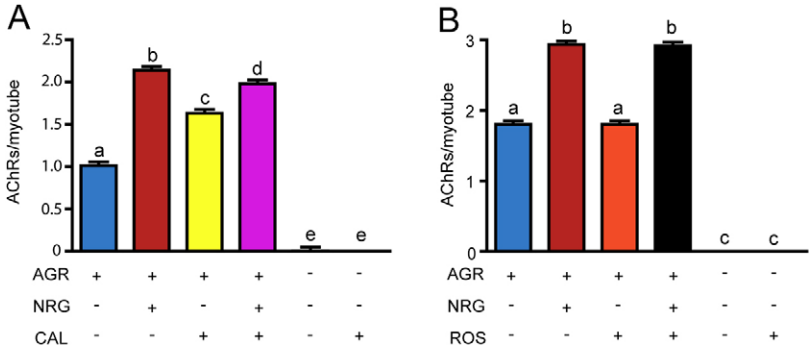

Fig. 6. Inhibitors of calpain and Cdk5 do not block potentiation of n-agrin AChR clustering by neuregulin. C2C12 myotubes were treated for 4 hours with n-agrin (AGR, 1 nM) with or without neuregulin-1 (NRG, 3 nM) in the presence or absence of inhibitors of calpain or roscovitine. (**A**) In the presence of the calpain inhibitor, calpeptin (CAL, 20 μM), neuregulin-1 was still able to potentiate n-agrin-induced AChR clustering (bars 3 and 4; $P<0.001$, $n=4$, ANOVA). (**B**) In the presence of the Cdk5 inhibitor roscovitine (ROS, 2 μM), potentiation by neuregulin-1 of n-agrin-induced AChR clustering was unimpaired (bars 2 and 4). Different lowercase letters indicate significant differences between groups with $P<0.001$. Values are means ± s.e.m.

therefore assessed the tyrosine phosphorylation of MuSK in response to a 20-minute treatment with 1 nM n-agrin with or without 3 nM neuregulin-1. MuSK was immunoprecipitated from cell lysates and the degree of MuSK phosphorylation was expressed as a percentage of phosphorylation in response to 10 nM n-agrin treatment (Fig. 7B).

As expected, MuSK phosphorylation was not detectable in control (untreated) myotubes (Fig. 7A, upper panel, lane 1; 7B, bar 5), whereas 1 nM n-agrin treatment induced MuSK phosphorylation (Fig. 7A, upper panel, lane 2; 7B, bar 2). Addition of 3 nM neuregulin-1 concurrently with 1 nM n-agrin further increased MuSK phosphorylation compared with myotubes treated with 1 nM n-agrin alone (Fig. 7A, upper panel, compare lanes 2 with 4; 7B, compare bars 2 and 3). Myotubes treated with neuregulin-1 alone showed no detectable MuSK phosphorylation (Fig. 7A, upper panel, lane 5; 7B, bar 4). These results confirm that n-agrin increases MuSK phosphorylation. Moreover, they show that when myotubes were treated with sub-maximal concentrations of n-agrin, neuregulin-1 was able to potentiate n-agrin-induced phosphorylation of MuSK, just as it is able to potentiate n-agrin-induced AChR clustering.

Blocking Shp2 function attenuates the potentiation of AChR clustering and MuSK phosphorylation by neuregulin-1

Recent studies have identified the protein tyrosine phosphatase Shp2 as a negative regulator of AChR clustering. Activation of MuSK by n-agrin led to the activation of Shp2, which then acted to repress excessive MuSK phosphorylation (Madhavan et al., 2005). We examined the effect of a 4-hour treatment with neuregulin-1 on n-agrin-induced AChR cluster formation in the presence of the Shp2 inhibitor, NSC-87877 (1 μM) (Chen et al., 2006) (Fig. 8A). As previously shown, after 4 hours in the continuous presence of n-agrin, 3 nM neuregulin-1 potentiated the number of large AChR clusters formed by 1 nM n-agrin (Fig. 8A, bars 1 and 2). Addition of the Shp2 inhibitor NSC-87877 alone did not cause AChR clustering (Fig. 8A, bar 6). However, in the presence of 1 nM n-agrin, NSC-87877 potentiated n-agrin-induced AChR clustering (Fig. 8A, compare bars 1 and 3). Furthermore, in the presence of NSC-87877, neuregulin-1 was unable to produce any further potentiation of n-agrin-induced AChR clustering (Fig. 8A, compare bars 3 and 4), thus the ability of neuregulin-1 to potentiate n-agrin-induced AChR clustering appears to depend upon the function of Shp2 phosphatase.

Because the Shp2 inhibitor NSC-87877 blocked neuregulin-1 potentiation of n-agrin-induced AChR clustering we examined its effect on MuSK phosphorylation. N-agrin causes rapid MuSK phosphorylation within 1 hour; long before AChR clustering reaches its maximal level at 4 hours (Fuhrer et al., 1997). We therefore examined MuSK phosphorylation in myotubes 20 minutes after the addition of n-agrin and/or neuregulin-1. MuSK phosphorylation was measured as a percentage of the phosphorylation in response to 1 nM n-agrin plus 3 nM neuregulin-1, designated a value of 100% (Fig. 8B, bar 2). Again, neuregulin-1 significantly increased the n-agrin-induced tyrosine phosphorylation of MuSK (Fig. 8B, compare bars 1 and 2); however, in the presence of NSC-87877 neuregulin-1 failed to potentiate n-agrin-induced MuSK phosphorylation (Fig. 8B, compare bars 2 and 4). Although NSC-87877 appeared to increase the mean levels of MuSK phosphorylation induced by either n-agrin or n-agrin plus neuregulin-1 (Fig. 8B, bars 3 and 4 respectively), this was less than that produced by n-agrin plus neuregulin-1 alone (Fig. 8B, compare bar 2 with bars 3 and 4). NSC-87877 alone did not cause detectable MuSK phosphorylation (Fig. 8B, bar 5). Together these results suggest that blocking Shp2 function with NSC-87877 (Zhao et al., 2007)

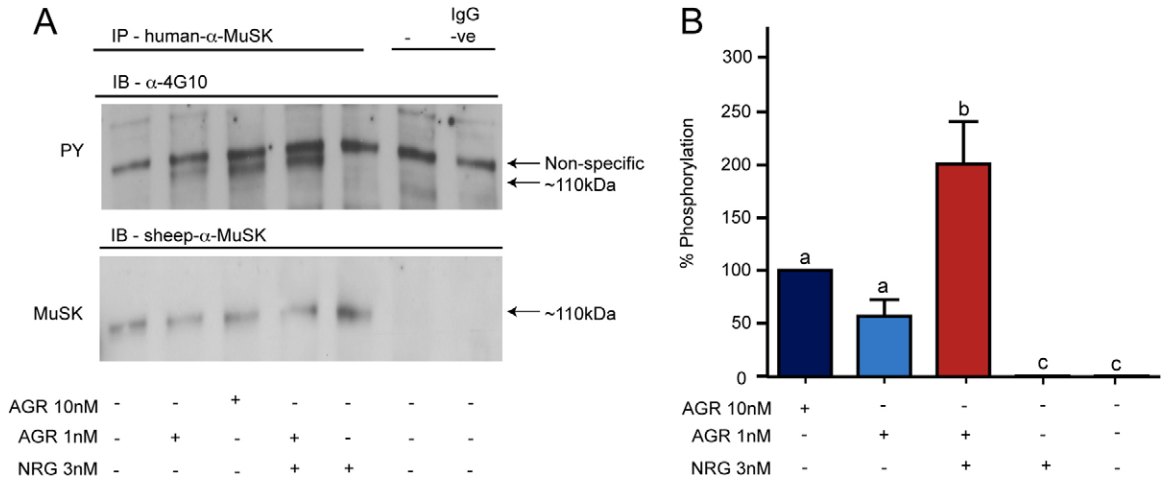

Fig. 7. Neuregulin-1 potentiates MuSK phosphorylation. C2C12 myotubes were treated for 20 minutes with n-agrin (AGR, 1 nM) with or without neuregulin-1 (NRG, 3 nM). (**A**) Sample blot showing tyrosine phosphorylation (PY ~110 kDa band; upper panel) of the MuSK band (lower panel). MuSK phosphorylation was increased in response to n-agrin treatment (upper panel, lane 2). Neuregulin-1 (3 nM) significantly potentiated n-agrin-induced (1 nM) MuSK phosphorylation (upper panel, compare lanes 2 and 4; $P<0.001$, $n=7$, ANOVA). No precipitating antibody (-ve ctrl, lane 6) and control human IgG (IgG -ve, lane 7) were included as negative controls. (**B**) Densitometric quantification of MuSK phosphorylation in response to a 20-minute treatment. Phosphorylation was detected with 4G10 and immunoblots were stripped and re-probed with anti-MuSK. The integrated pixel intensity value for each phosphorylation band (upper panel in A) was first normalized to the MuSK protein band (lower panel in A). The normalized integrated pixel values were then compared with the integrated pixel value of the 10 nM n-agrin-induced MuSK phosphorylation band (designated a value of 100% MuSK phosphorylation). Note the 'Non specific' band was routinely detected under all conditions. Different lowercase letters indicate significant differences between groups; $P<0.05$ between a and c, and $P<0.001$ when comparing b with a and c. Values are means ± s.e.m.

inhibits the potentiation of AChR clustering and MuSK phosphorylation by neuregulin-1.

Discussion

In this study we aimed to clarify the actions of neuregulin-1 on n-agrin-induced AChR clustering and the underlying molecular mechanism. We showed that the ability of neuregulin-1 to potentiate AChR clustering requires that myotubes be simultaneously exposed to neuregulin-1 and n-agrin. The potentiation did not involve elevated expression of AChRα or MuSK mRNAs, rather neuregulin-1 potentiated the tyrosine phosphorylation of MuSK, a key determinant of downstream AChR clustering. Neuregulin-1 potentiation of MuSK phosphorylation and downstream AChR cluster formation were both blocked by an inhibitor of the tyrosine phosphatase, Shp2, a known modulator of AChR clustering (Camilleri et al., 2007; Madhavan et al., 2005; Zhao et al., 2007). Neuregulin-1 was able to potentiate AChR clustering both in primary cultured muscle cells and when injected into embryonic muscles in utero suggesting that the proposed pathway is physiologically relevant.

Neuregulin-1 enhanced AChR cluster formation in embryonic muscles in vivo and in vitro, presumably through the ErbB2 receptor (Fig. 1A–C; Fig. 4). Injection of neuregulin-1 into sternomastoid muscles of E15 mouse embryos resulted in a marked increase in AChR cluster size (4 hours post injection) compared with control injected embryos. There was a significant increase in the largest class of AChR clusters, consistent with the increase in the number of large AChR clusters that we quantified on cultured myotubes. Our rationale for injecting neuregulin-1 at E15 was based on the immaturity of the neuromuscular synapse. E15 is the stage at which neuromuscular synapse formation begins, a process that is characterized by the appearance of MuSK and small diffuse AChR clusters (Bowen et al., 1998; Noakes, 1999; Noakes et al., 1993). At this stage agrin is 'diffusely distributed' on the muscle surface (Hoch et al., 1993), before becoming increasingly concentrated within the synaptic cleft at later stages (Hoch, 1999; Hoch et al., 1993; Magill-Solc and McMahan, 1990). Neuregulin-1 is expressed by embryonic muscle and motor nerve terminals (Loeb, 2003; Loeb et al., 1999; Meyer et al., 1997). The cognate ErbB receptors are localized both on the postsynaptic membrane (ErbB2, ErbB3 and ErbB4) and on Schwann cells (ErbB3) at developing neuromuscular synapses (Moscoso et al., 1995; Trinidad et al., 2000; Zhu et al., 1995). We have shown by immunostaining that ErbB2 occurs synaptically (co-extensive with AChRs) and extra-synaptically on the muscle surface, at E15 (Fig. 1A–C).

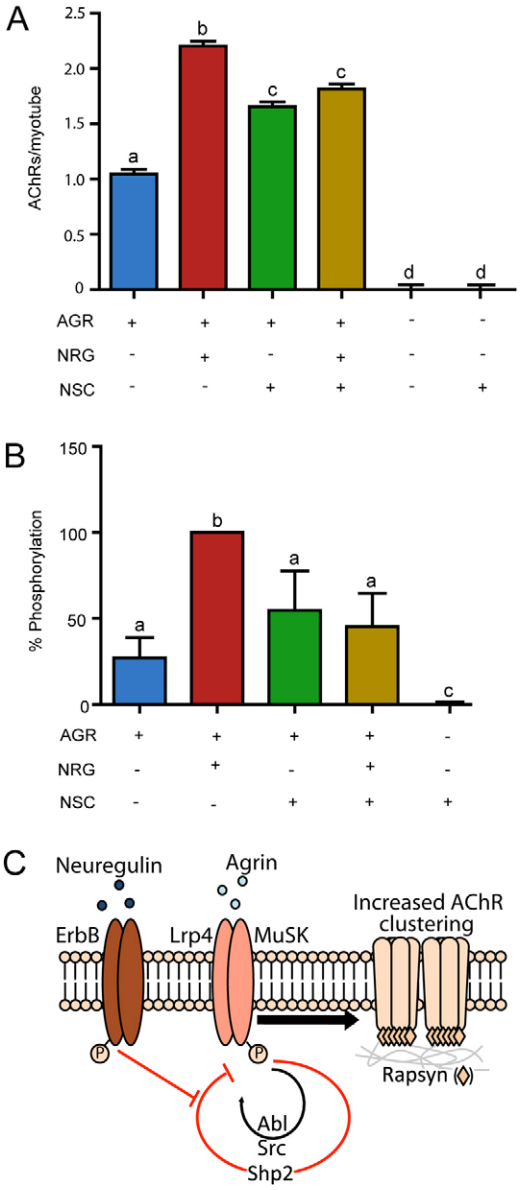

Fig. 8. Blocking Shp2 function attenuates the potentiation of AChR clustering and MuSK phosphorylation by neuregulin-1. C2C12 myotubes were treated with n-agrin (AGR, 1 nM) with or without neuregulin-1 (NRG, 3 nM) in the presence or absence of a Shp2 inhibitor (NSC; NSC-87877, 1 μM). (**A**) Myotubes treated for 4 hours with n-agrin plus neuregulin-1 led to a potentiation in AChR cluster number compared to n-agrin treatment alone (bars 1 and 2). In the presence of the Shp2 inhibitor, neuregulin-1 was no longer able to potentiate n-agrin-induced AChR clusters (compare bar 2 with bars 3 and 4). Different lowercase letters indicate significant differences between groups; $P<0.001$, $n=3$, ANOVA. Values are means ± s.e.m. (**B**) Densitometric quantification of MuSK phosphorylation after treatment of myotubes for 20 minutes with n-agrin plus neuregulin-1. The integrated pixel value for each phosphorylation band was normalized to MuSK protein expression then compared with the integrated pixel value of the 1 nM n-agrin plus 3 nM neuregulin-1-induced MuSK phosphorylation band (designated a value of 100% MuSK phosphorylation; bar 2). Treatment of myotubes with 1 nM n-agrin and 3 nM neuregulin-1 resulted in a significant increase in MuSK phosphorylation compared with 1 nM n-agrin treatment alone (bars 1 and 2; $P<0.05$, $n=3$, ANOVA). In the presence of NSC-87877, neuregulin-1 could no longer potentiate n-agrin-induced MuSK phosphorylation (compare bar 2 to bars 3 and 4; $P<0.05$, $n=3$, ANOVA). The Shp2 inhibitor alone did not induce MuSK phosphorylation (bar 5). Different lowercase letters indicate significant differences between groups. Values are means ± s.e.m. (**C**) A hypothetical model for the potentiation of n-agrin-induced AChR clustering by neuregulin-1. At the neuromuscular synapse, n-agrin binds to the Lrp4–MuSK complex, leading to MuSK phosphorylation. Abl and Src kinases help maintain MuSK phosphorylation levels (Finn et al., 2003; Smith et al., 2001). Shp2 tyrosine phosphatase dephosphorylates MuSK (Madhavan and Peng, 2005; Madhavan et al., 2005). When ErbB is activated by neuregulin-1, Shp2 binds to the ErbB complex (Tanowitz et al., 1999). We hypothesize that this interaction of Shp2 with activated ErbB sequesters Shp2 in such a way as to block the de-phosphorylation of MuSK. This results in higher levels of n-agrin-induced MuSK phosphorylation.

By contrast, ErbB3 staining appeared to be restricted to the synaptic region of the developing neuromuscular synapse, consistent with its pre-and post-synaptic distributions (Fig. 1D–F). ErbB2 staining was also detected on cultured muscle cells (Fig. 4A). Although we cannot rule out a possible indirect effect of neuregulin-1 acting through terminal Schwann cells in vivo, this could not explain the ability of neuregulin-1 to potentiate AChR clustering on isolated muscle cells in culture. The ability of injected neuregulin-1 to increase AChR cluster size in vivo suggests that MuSK activation by n-agrin is likely to be sub-maximal at these early developing synapses. This assumption is supported by our in vitro experiments, in which we have used a sub-maximal dose of n-agrin, to demonstrate potentiation of n-agrin-mediated AChR clustering by neuregulin-1.

Our live imaging results confirm that AChR cluster formation is a multi-stage, reversible process. Formation of multiple small AChR clusters (<25 μm long) was followed by their coalescence into large, continuous AChR clusters (≥25 μm long) 2–6 hours after the addition of n-agrin (Fig. 2A). In the continual presence of n-agrin for 12 hours, large AChR clusters were seen to break up into several smaller AChR clusters before finally dissipating (Fig. 2). The initial AChR cluster assembly depends upon MuSK kinase activation and rapsyn (DeChiara et al., 1996; Gautam et al., 1995; Ghazanfari et al., 2010; Sanes and Lichtman, 2001; Strochlic et al., 2005). The later process of fragmentation might involve other intracellular signaling systems with the potential to cause AChR cluster dispersal (e.g. Shp2 and/or calpain-dependent mechanisms) (Chen et al., 2007; Ghazanfari et al., 2010; Wu et al., 2010; Zhao et al., 2007). Previous studies have shown that the maximal number of n-agrin-induced AChR clusters reached a peak at 4–6 hours after the addition of n-agrin to the myotube culture (Ferns et al., 1996; Ngo et al., 2004). During the first 4 hours of n-agrin exposure, AChR cluster coalescence events predominated (Fig. 2). The previously reported decline in large AChR cluster numbers after 4 hours could be explained by an increase in the frequency of fragmentation events (4–8 hours) and a subsequent drop in the rate of coalescence events (in the last 4 hours of n-agrin exposure). It is interesting to note instances where a large AChR cluster reassembled after breaking up (five of nine clusters). This suggests there is competition between simultaneous processes of assembly and fragmentation. Potentiation by neuregulin-1 of the early-phase of AChR clustering in C2C12 myotubes occurred only in the presence of n-agrin, suggesting that it relies upon the interaction of short-lived signaling events initiated by n-agrin and neuregulin-1.

In vitro, neuregulin-1 potentiation of n-agrin-induced AChR clustering did not appear to involve its well-established function of activation of synaptic gene transcription. Neuregulin-1 is reported to induce AChRε and AChRδ subunit gene transcription when added to cultures of mouse myotubes. In chick myotubes it is also reported to induce expression of the AChRα subunit and MuSK genes (Fu et al., 1999; Ip et al., 2000; Martinou et al., 1991; Ngo et al., 2004). N-agrin has also been reported to induce the transcription of *Musk* indirectly by recruiting ErbB receptors into muscle membrane (Lacazette et al., 2003); however, upregulation of these genes was either studied in an avian system or with treatments of 24 hours or longer when studied in mammalian myotubes (Fu et al., 1999; Ip et al., 2000; Lacazette et al., 2003; Li and Loeb, 2001; Martinou et al., 1991; Ngo et al., 2004). This might explain why we found no increase in the expression of the AChRα subunit and MuSK genes in mouse C2C12 myotubes after just 4 hours. Although we have not examined expression of all synaptic genes, the results with MuSK and AChRα argue against the idea that neuregulin-1 potentiates n-agrin-induced AChR clustering through its known pathway for enhancing synaptic gene transcription (Sanes and Lichtman, 2001).

The phosphorylation of MuSK in response to n-agrin appears to be moderated by a balance of protein tyrosine kinases and phosphatases (Camilleri et al., 2007; Finn et al., 2003; Madhavan and Peng, 2005; Zhao et al., 2007). We found that the Shp2 inhibitor NSC-87877 blocked the potentiation of n-agrin-induced clustering by neuregulin-1. One interpretation involves the previously hypothesized negative feedback pathway involving Src, SIRP and Shp2 (Madhavan and Peng, 2005; Zhao et al., 2007). N-agrin binding to the MuSK complex leads to tyrosine phosphorylation of SIRPα1 through Src and possibly other tyrosine kinases. Phosphorylated SIRPα1 in turn activates Shp2 (Zhao et al., 2007), activated Shp2 then serves to limit the extent of n-agrin-induced MuSK phosphorylation (Madhavan et al., 2005). We propose that neuregulin-1 treatment potentiates n-agrin-induced AChR clustering by somehow suppressing this negative feedback loop (Fig. 8C). In support of this idea, inhibition of Shp2 with NSC-87877 ablated the ability of neuregulin-1 to potentiate n-agrin-induced MuSK phosphorylation. However, we have not directly measured the effects of sub-maximal concentrations of n-agrin (with and without neuregulin-1) upon Shp2 activity in embryonic muscle cells. In addition, other studies have shown that NSC-87877, in the concentration range of 0.2–1 μM might also inhibit Shp1 (Qian et al., 2008). Further studies are needed to clarify the mode of this proposed inhibition.

The mechanism by which prolonged neuregulin-1 exposure might accelerate AChR cluster dispersal remains less clear. Earlier work showed that chronic administration of neuregulin-1 can lead to loss of postsynaptic AChRs at NMJs (Trachtenberg and Thompson, 1997), and recent studies have shown that continued activation of ErbB2 receptors in muscle is sufficient to cause the loss of n-agrin-induced AChR clusters (Ponomareva et al., 2006). In agreement with previous studies implicating Cdk5 in AChR cluster disassembly (Ip et al., 2000; Lin et al., 2005), blocking Cdk5 function with roscovitine partially rescued overnight neuregulin-1-driven AChR cluster dispersal (data not shown). We also tested the effect of inhibiting calpain and Shp2 (Chen et al., 2007; Madhavan et al., 2005; Zhao et al., 2007), but such inhibitors had no effect upon neuregulin-1-induced AChR cluster dispersal at the 12-hour time-point (data not shown). Hence, the long-term action of neuregulin-1 on n-agrin-induced AChR cluster dispersal will require further detailed study.

Fig. 8C summarizes a hypothetical pathway by which neuregulin-1 might potentiate MuSK activation. Synaptic neuregulin-1 acts through ErbB receptors on the muscle cell surface, whereas n-agrin activates postsynaptic MuSK. Abl and Src kinases provide positive feedback to sustain the phosphorylation and kinase activity of MuSK. Shp2 phosphatase is also activated downstream of MuSK, but functions to limit the extent of MuSK phosphorylation (Madhavan and Peng, 2005). Shp2 occurs in the postsynaptic membrane but when ErbB is activated by neuregulin-1, Shp2 binds to the ErbB complex (Tanowitz et al., 1999). We hypothesize that the interaction of Shp2 with activated ErbB sequesters Shp2 in such a way as to block MuSK

dephosphorylation (Fig. 8C), resulting in higher levels of n-agrin-induced MuSK phosphorylation.

Neuregulin-1 potentiation of MuSK-mediated AChR clustering appears to play a minor role in early development of the NMJ. When the neuregulin-1 gene was inactivated in both nerve and muscle, AChR clusters still formed but nerve terminals withdrew and postsynaptic AChRs were slightly reduced compared with control embryos (Jaworski and Burden, 2006). It is possible that the reduction in AChRs in the absence of synaptic neuregulin-1 might have been an indirect consequence of the withdrawal of the nerve terminal. This cannot fully explain the acute growth of AChR clusters (<4 hours) when we injected neuregulin-1 into muscles of wild-type embryos, nor can it explain the gradual loss of AChR clusters from the NMJ when neuregulin-1 was chronically administered to adult wild-type mice over 5 days (Trachtenberg and Thompson, 1997). Muscle-specific targeting of the ErbB receptor 2 and 4 genes was consistent with endogenous neuregulin-1 acting postsynaptically to enhance AChR clustering, albeit modestly (Escher et al., 2005; Leu et al., 2003). Targeting of the Shp2 gene in muscle did not produce any detectable change in AChR cluster size (Dong et al., 2006). A caveat noted by Dong et al. was that gene targeting did not completely eliminate Shp2 expression in muscles. Indeed it can be difficult to be sure of complete inactivation of any gene in multinucleated muscle fibres (Jaworski et al., 2007; O'Leary et al., 2007). Expression of the Cre recombinase gene was often insufficient to completely excise *loxP*-targeted genes, such as *Shp2*, *ErbB2* and *ErbB4* in multinucleated muscle cells (Dong et al., 2006; Escher et al., 2005; Jaworski and Burden, 2006; Leu et al., 2003), and studies that target the inactivation of genes in specific cells types (such as motor nerve and muscle) do not address acute action and/or actions of neuregulin-1 at later stages of NMJ development. This latter point is worth noting, given that both n-agrin and neuregulin-1 become concentrated in the synaptic basal lamina of the NMJ after birth (Hoch et al., 1993; Moscoso et al., 1995).

Although neuregulin-1 signaling appears to be non-essential for the early development of the NMJ, the NMJ continues active regeneration throughout life and in response to challenges such as micro-denervation and reinnervation in situations where MuSK signaling might not be optimal (Cole et al., 2010; Valdez et al., 2010; Wilson and Deschenes, 2005). The ability of the postsynaptic membrane to respond optimally to such challenges could well involve convergence of n-agrin and neuregulin-1 signaling.

Materials and Methods

Ethical approval

Experiments complied with the policies and regulations regarding animal experimentation and other ethical matters (Drummond, 2009). Experiments were approved by the University of Queensland Animal Ethics Committee and were in accordance with the Queensland Government Animal Research Act 2001, associated Animal Care and Protection Regulations (2002 and 2008), as well as the Australian Code of Practice for the Care and Use of Animals for Scientific Purposes, 7th Edition (National Health and Medical Research Council, 2004).

Reagents

The C2C12 cell line was obtained from the European Collection of Cell cultures (www.ecacc.org.uk; GBR). Recombinant rat neural-agrin (amino acids 1153–1959) (Rupp et al., 1992) was purchased from R&D Systems (Minneapolis, MN). A dose–response assay was conducted for the n-agrin used in this study. Half-maximal AChR clustering after 4 hours exposure was obtained with approximately 1 nM n-agrin, and 10 nM yielded the maximum number of AChR clusters. Recombinant human heregulin-β1 (neuregulin-1) consisting of the 30 kDa extracellular domain (amino acids 1–241) was obtained from Thermo Scientific (Waltham, MA). Calpeptin was bought from Merck (Whitehouse Station, NJ) and used to inhibit calpain (Chen et al., 2007). Roscovitine (from Merck) was used to inhibit Cdk5 (Lin et al., 2005). NSC-87877, a Shp2 inhibitor (Chen et al., 2006) was obtained from Merck (Zhao et al., 2007). PD168393 was purchased from Merck and used to inhibit ErbB2 (Calvo et al., 2011). Tetramethylrhodamine isothiocyanate (TRITC)-conjugated α-bungarotoxin (TRITC–α-BTX; Sigma, St. Louis, MO) was used at 1:10,000 in differentiation medium. Affinity purified human MuSK autoantibodies, and sheep anti-MuSK antibodies were used as described previously (Cole et al., 2010). Other antibodies used in this study were: monoclonal anti-mouse phosphotyrosine 4G10 (1:1000: Millipore, Billerica, MA); rabbit anti-sheep IgG HRP (1:2000; Sigma); sheep anti-mouse IgG HRP (1:10,000: Amersham/GE Healthcare Bio-Sciences Corp., Piscataway, NJ); rabbit anti-bovine neurofilament 200 (1:1000, Sigma); rabbit anti-human synaptophysin (1:50, DakoCytomation, Glostrup, Denmark); rabbit anti-ErbB2 and rabbit anti-ErbB3 (1:100; Santa Cruz Biotechnology, Santa Cruz, CA); Alexa-Fluor-488-conjugated goat anti-rabbit IgG (1:500 to 1:5000) and Alexa-Fluor-555–α-BTX (1:500) from Invitrogen (Victoria, Australia). For immunostaining experiments, antibodies were diluted in 2% bovine serum albumin (BSA) in Triton X-100 in PBS, pH 7.4, and for western blot experiments in 2.5% skimmed milk in 0.05% Tween 20 in Tris-buffered saline (TBS-T), pH 7.6.

Muscle cell culture and assays

Mouse C2C12 cells and C57Bl/6J mouse primary myotubes were maintained at 37℃ in 5% CO_2 and cultured as previously described (Gautam et al., 1996; Han et al., 1999; Ngo et al., 2004). The AChR clusters that appeared on C2C12 and primary myotubes were labelled with TRITC–α-BTX (1:10,000) and quantified according to previous guidelines (Gee et al., 1994; Ngo et al., 2004). Specifically, only AChR clusters ≥25 μm in their longest dimension were counted. AChR counts represent the number of AChR clusters per myotube segment, as per our previous studies. In all bioassays, treatment with n-agrin and neuregulin-1 involved the addition of neuregulin-1 in the continued presence of n-agrin unless otherwise stated. Statistical significance was determined by analysis of variance (ANOVA) with Bonferroni post-hoc tests (Statgraphics Plus 3.0, Statistical Graphics Corp., VA). Graphs were constructed in Prism 4.01 (GraphPad Software Inc., CA).

For time-lapse imaging of AChRs, C2C12 myotubes grown on 6 cm plastic plates were imaged in a 37℃, 5% CO_2 humidified chamber. Cells were imaged under a 10× (NA 0.3) EC Neofluar objective on an Axio-Observer Z1 inverted microscope using a DSRed43 reflector (Carl Zeiss Inc., Oberkochen, Germany). Cells were treated with 10 nM n-agrin to induce AChR clustering. TRITC–α-BTX (1:10,000) was added at the same time as n-agrin. Time-lapse images were captured on an Axiocam MR3 camera (Carl Zeiss Inc.) at 10-minute intervals for 12 hours over six random fields within each experiment. AChRs were considered to be a large AChR cluster when they were ≥25 μm in their longest dimension (i.e. continual staining of the longest dimension in the cluster).

For ErbB2 staining, C2C12 myotubes were grown on glass coverslips in 24-well plates. Myotubes were treated with 1 nM n-agrin for 4 hours prior to incubation with Alexa-Fluor-555–α-BTX (1:500) for 1 hour at 37℃ in 5% CO_2. Cells were washed twice with room-temperature PBS prior to fixation with 4% paraformaldehyde–phosphate buffer for 5 minutes at room temperature. Cells were washed twice with room-temperature PBS and blocked for 30 minutes with 2% BSA–PBS–0.05% Tween 20. Myotubes were incubated overnight at 4℃ with rabbit anti-ErbB2 (1:100). Cells were washed three times with room-temperature PBS prior to incubation with Alexa-Fluor-488-conjugated goat anti-rabbit IgG (1:500) for 1.5 hours at room temperature. They were then washed a further three times with room-temperature PBS before being mounted with Prolong Gold anti-fade (Invitrogen). The negative control for rabbit ErbB2 receptor primary antibody staining in C1C12 myotubes was obtained by omission of the primary antibody and incubation with an Alexa-Fluor-488-conjugated goat anti-rabbit IgG secondary antibody (supplementary material Fig. S2). ErbB2 and AChRs were imaged using a Zeiss LSM Meta 510 upright confocal microscope with a Plan-Apochromat 63× (NA 1.4) oil objective (Carl Zeiss Inc.).

MuSK immunoprecipitation

Immunoprecipitation of MuSK was conducted as previously described (Cole et al., 2010). C2C12 myotubes that were grown on 6 cm plates were lysed (50 mM Tris-HCl, 150 mM NaCl, 0.1% SDS, 2 mM EDTA, 10 mM NaF, 10 mM $Na_4P_2O_4$, 1 mM Na_3VO_4, 1% NP40 and protease inhibitor; cat. no. 836170001, Roche, Basel, Switzerland) and pre-cleared before coupling MuSK to 10 μl affinity purified human anti-human MuSK, per sample. The antigen complex was precipitated with 50 μl protein-G–Sepharose beads. Pellets were washed three times in lysis buffer: once with 1 M NaCl buffer, once with no NaCl buffer and once in 50 mM Tris (pH 8). Samples were resolved by SDS-PAGE and transferred to nitrocellulose membranes. Membranes were blocked in 2% BSA–TBS-T and incubated overnight with anti-phosphotyrosine antibody, 4G10 (1:1000 in 1% BSA–TBS-T). Anti-4G10 was detected with sheep anti-mouse IgG HRP (1:10,000 in 1% BSA–TBS-T). Blots were stripped and re-probed with affinity-purified sheep anti-MuSK (1:125 in 2.5% skimmed milk in TBS-T) and detected with rabbit anti-sheep IgG HRP (1:2000 in 2.5% skimmed milk in TBS-T) to verify

equal loading of MuSK protein. Controls included omission of anti-MuSK antibody from the immunoprecipitation step and substitution of control human IgG (10 mg/ml).

Densitometric analyses of immuno-reactive bands were carried out using ImageJ software (Abramoff et al., 2004). The integrated pixel value of each protein band was obtained by multiplying its intensity value by its area value. The integrated pixel value for each protein band was first normalized to that of the corresponding immuno-band stained for MuSK. The normalized integrated pixel values were then compared with the integrated pixel value of the MuSK phosphorylation band that was induced by maximal (10 nM n-agrin) treatment (designated a value of 100% MuSK phosphorylation in Fig. 7B) or the integrated pixel value of the MuSK phosphorylation band that was induced by 1 nM n-agrin with 3 nM neuregulin-1 (designated a value of 100% in Fig. 8B). Data were analyzed using ANOVA with Bonferroni post-hoc tests, and graphs were constructed in Prism 4.01 (GraphPad Software Inc.).

Quantitative real-time PCR

RNA was extracted and prepared from myotubes grown on 6 cm plates using an RNeasy Mini Kit (Qiagen, Hilden, Germany) according to the manufacturer's instructions. Reverse transcription, primer selection and quantitative real-time PCR for the AChRα subunit and MuSK RNAs were preformed as previously described (Cole et al., 2010). The identity of the PCR products was confirmed by agarose gel electrophoresis and sequencing.

Ultrasound-guided microinjections

Time-mated C57Bl/6 female mice from University of Queensland Biological Resource animal house were anaesthetized with isoflurane (Provet, QLD, Australia) in oxygen (1.5–2% induction and maintenance) through a nose cone, and anaesthesia was assessed and monitored by suppression of the foot-withdrawal reflex. E15 embryos were imaged by micro-ultrasound (Vevo-770™, VisualSonics, Ontario, Canada) in real-time. Microinjection experiments performed with the aid of a microinjection rail system and 40 MHz transducer probe (RMV711, VisualSonics), were modified from the method described previously (Slevin et al., 2006). The mother's abdominal cavity was opened to allow access to each uterine horn. PBS or neuregulin-1 (33 nM) mixed with fluorescent beads (Fluoresbrite® yellow–green microspheres, 2 µm diameter; Polysciences Inc., Warrington, PA) was administered (690 nl to 1 µl) to the sternomastoid muscle at 69 nl/second (Nanoject II, Drummond Scientific Company, Broomall, PA) per embryo. The mother's abdominal cavity was sutured closed after all embryos were micro-injected. Buprenorphine diluted in saline was administered (0.1 mg/kg, subcutaneous) to the mother for pain management. Mothers were killed 4 hours post microinjection. Mice were first rendered unconscious by anaesthesia (2.5 mg ketamine and 0.5 mg Xylazine per 20 g mouse, intraperitoneally) followed by cervical dislocation after the foot-withdrawal reflex was completely suppressed. Two adult females were used in this study. Embryos were dissected, anaesthetized on ice and killed by exposure of the thoracic cavity. The shoulders and head of each embryo were dissected and mounted in optimal cutting temperature medium (OCT, Sakura, Tokyo, Japan). A total of 12, E15 embryos were used.

Microscopy and quantification of ErbB, muscle fiber area, AChRs and innervation

For ErbB2 and ErbB3 receptors, E15 sternomastoid muscles were fixed in 4% paraformaldehyde–phosphate buffer for 40 minutes at room temperature and washed three times for 10 minutes with PBS. Cryosections (16 µm thick) were obtained and stored at −20℃. Sections were blocked with 2% goat serum, 0.5% BSA and 0.5% Triton X-100 in PBS for 30 minutes. Sections were incubated with ErbB2 or ErbB3 antibodies (1:100; Santa Cruz) overnight at 4℃ and probed for with an Alexa-Fluor-488-conjugated goat anti-rabbit IgG (1:5000; Invitrogen). Alexa-Fluor-555–α-BTX (1:5000; Molecular Probes) was added to the secondary antibody mix to detect AChRs. Negative controls for rabbit ErbB2 and rabbit ErbB3 receptor primary antibody staining of embryonic muscle were obtained by omission of the primary antibody and incubation with an Alexa-Fluor-488-conjugated goat anti-rabbit IgG secondary antibody (supplementary material Fig. S2). Sections were imaged using a Zeiss LSM Meta 510 upright confocal microscope using a Plan-Apochromat 63× (NA1.4) oil objective (Carl Zeiss Inc.).

For AChRs, samples were incubated with Alexa-Fluor-555–α-BTX (1:500) for 1 hour at room temperature, washed three times, for 10 minutes each, with PBS, and mounted with FluoroGuard™ Anti-Fade Reagent (Bio-Rad, CA, USA). Cryosections were imaged under a Zeiss LSM Meta 510 upright confocal microscope using a Plan-Apochromat 20× (NA 0.8) air objective (Carl Zeiss Inc.). To avoid biased sampling, AChRs were examined 100 µm above and below the point of highest injected bead concentration (this point was assumed to have the highest concentration of injectate). AChR clusters were imaged from an area in each section that contained the highest number of AChRs. Single optical plane images were collected for each section. The area and number of AChRs was measured by ImageJ. The 'analyze particles' plugin was used to quantify the areas and mean pixel intensities for the isolated AChRs. AChRs included for analysis were greater than 50 pixels. Areas of AChR clusters were converted from pixels into micrometers squared and frequency histograms were produced in Prism 4.01 (GraphPad Software Inc.) with bin values set at multiples of 5 μm^2 from 0 to 50 μm^2. All AChR clusters above 50 μm^2 were binned into a 50+ group. Statistical differences were calculated using the Mann–Whitney *U*-test.

To assess muscle fiber diameter, samples were incubated with Alexa-Fluor-555–α-BTX (1:500) as described above, and mounted with FluoroGuard™ Anti-Fade Reagent (Bio-Rad). Cryosections were viewed under TRITC and FITC (fluorescein isothiocyanate) optics with a 40× (NA 0.85) air objective on an Olympus BX60 microscope. The section that contained the highest bead density was selected from each injected embryo. A random area (containing AChRs) was captured with a Zeiss AxioCam MRm camera. Twenty muscle fibers in each section were randomly selected and cross sectional area (in pixels) of each selected muscle fiber was measured using ImageJ software. The average muscle fiber cross sectional area of PBS-injected embryos was compared with that of neuregulin-1-injected embryos using an unpaired *t*-test and Prism 4.01 (GraphPad Software Inc.).

To assess the innervation status of AChR clusters in the injected muscles, the coverslips were removed from the same sections, which were then immunostained for the presence of motor axons and their terminal endings with a neurofilament (1:1000: Sigma) and synaptophysin (1:50: DakoCytomation) primary antibody mixture and probed for with an Alexa-Fluor-488-conjugated goat anti-rabbit IgG (1:500) as described previously (Banks et al., 2005). Alexa-Fluor-555–α-BTX (1:500) was added to the second antibody mix to ensure no loss of AChR labelling. Sections were imaged using an Axio Imager 319 microscope (Carl Zeiss Inc.). The number of AChRs associated with nerves (i.e. ≤5 µm away) by positive neurofilament–synaptophysin staining was scored over the total number of AChR clusters in the randomly selected area (the area with the greatest number of AChR clusters). Statistical analyses were performed using unpaired *t*-tests in Prism 4.01 (GraphPad Software Inc.).

Acknowledgements

We thank D. Muller for her assistance at the Queensland Brain Institute Zeiss imaging suite, N. Ghazanfari (Bosch Institute) for her assistance with protein biology, M. White for assistance with tissue culture, F. Steyn for his assistance and P. McCombe for critical reading of the manuscript.

Funding

This work was supported by the National Health and Medical Research Council of Australia [grant numbers 569680 and 570930 to P.G.N. and W.D.P.]; and a postgraduate scholarship from the University of Queensland (to S.T.N.).

Supplementary material available online at
http://jcs.biologists.org/lookup/suppl/doi:10.1242/jcs.095109/-/DC1

References

Abramoff, M. D., Magelhaes, P. J. and Ram, S. J. (2004). Image processing with ImageJ. *Biophotonics International* **11**, 36-42.

Banks, G. B., Kanjhan, R., Wiese, S., Kneussel, M., Wong, L. M., O'Sullivan, G., Sendtner, M., Bellingham, M. C., Betz, H. and Noakes, P. G. (2005). Glycinergic and GABAergic synaptic activity differentially regulate motoneuron survival and skeletal muscle innervation. *J. Neurosci.* **25**, 1249-1259.

Bowen, D. C., Park, J. S., Bodine, S., Stark, J. L., Valenzuela, D. M., Stitt, T. N., Yancopoulos, G. D., Lindsay, R. M., Glass, D. J. and DiStefano, P. S. (1998). Localization and regulation of MuSK at the neuromuscular junction. *Dev. Biol.* **199**, 309-319.

Brenner, H. R., Witzemann, V. and Sakmann, B. (1990). Imprinting of acetylcholine receptor messenger RNA accumulation in mammalian neuromuscular synapses. *Nature* **344**, 544-547.

Calvo, M., Zhu, N., Grist, J., Ma, Z., Loeb, J. A. and Bennett, D. L. (2011). Following nerve injury neuregulin-1 drives microglial proliferation and neuropathic pain via the MEK/ERK pathway. *Glia* **59**, 554-568.

Camilleri, A. A., Willmann, R., Sadasivam, G., Lin, S., Ruegg, M. A., Gesemann, M. and Fuhrer, C. (2007). Tyrosine phosphatases such as SHP-2 act in a balance with Src-family kinases in stabilization of postsynaptic clusters of acetylcholine receptors. *BMC Neurosci.* **8**, 46.

Chen, F., Qian, L., Yang, Z. H., Huang, Y., Ngo, S. T., Ruan, N. J., Wang, J., Schneider, C., Noakes, P. G., Ding, Y. Q. et al. (2007). Rapsyn interaction with calpain stabilizes AChR clusters at the neuromuscular junction. *Neuron* **55**, 247-260.

Chen, L., Sung, S. S., Yip, M. L., Lawrence, H. R., Ren, Y., Guida, W. C., Sebti, S. M., Lawrence, N. J. and Wu, J. (2006). Discovery of a novel shp2 protein tyrosine phosphatase inhibitor. *Mol. Pharmacol.* **70**, 562-570.

Chu, G. C., Moscoso, L. M., Sliwkowski, M. X. and Merlie, J. P. (1995). Regulation of the acetylcholine receptor epsilon subunit gene by recombinant ARIA: an in vitro model for transynaptic gene regulation. *Neuron* **14**, 329-339.

Cohen, M. W. and Godfrey, E. W. (1992). Early appearance of and neuronal contribution to agrin-like molecules at embryonic frog nerve-muscle synapses formed in culture. *J. Neurosci.* **12**, 2982-2992.

Cole, R. N., Ghazanfari, N., Ngo, S. T., Gervasio, O. L., Reddel, S. W. and Phillips, W. D. (2010). Patient autoantibodies deplete postsynaptic muscle-specific kinase leading to disassembly of the ACh receptor scaffold and myasthenia gravis in mice. *J. Physiol.* **588**, 3217-3229.

DeChiara, T. M., Bowen, D. C., Valenzuela, D. M., Simmons, M. V., Poueymirou, W. T., Thomas, S., Kinetz, E., Compton, D. L., Rojas, E., Park, J. S. et al. (1996). The receptor tyrosine kinase MuSK is required for neuromuscular junction formation in vivo. *Cell* **85**, 501-512.

Dong, X. P., Li, X. M., Gao, T. M., Zhang, E. E., Feng, G. S., Xiong, W. C. and Mei, L. (2006). Shp2 is dispensable in the formation and maintenance of the neuromuscular junction. *Neurosignals* **15**, 53-63.

Drummond, G. B. (2009). Reporting ethical matters in the Journal of Physiology: standards and advice. *J. Physiol.* **587**, 713-719.

Escher, P., Lacazette, E., Courtet, M., Blindenbacher, A., Landmann, L., Bezakova, G., Lloyd, K. C., Mueller, U. and Brenner, H. R. (2005). Synapses form in skeletal muscles lacking neuregulin receptors. *Science* **308**, 1920-1923.

Ferns, M., Deiner, M. and Hall, Z. (1996). Agrin-induced acetylcholine receptor clustering in mammalian muscle requires tyrosine phosphorylation. *J. Cell Biol.* **132**, 937-944.

Fertuck, H. C. and Salpeter, M. M. (1974). Localization of acetylcholine receptor by 125I-labeled alpha-bungarotoxin binding at mouse motor endplates. *Proc. Natl. Acad. Sci. USA* **71**, 1376-1378.

Fertuck, H. C. and Salpeter, M. M. (1976). Quantitation of junctional and extrajunctional acetylcholine receptors by electron microscope autoradiography after 125I-alpha-bungarotoxin binding at mouse neuromuscular junctions. *J. Cell Biol.* **69**, 144-158.

Finn, A. J., Feng, G. and Pendergast, A. M. (2003). Postsynaptic requirement for Abl kinases in assembly of the neuromuscular junction. *Nat. Neurosci.* **6**, 717-723.

Fricker, F. R., Lago, N., Balarajah, S., Tsantoulas, C., Tanna, S., Zhu, N., Fageiry, S. K., Jenkins, M., Garratt, A. N., Birchmeier, C. et al. (2011). Axonally derived neuregulin-1 is required for remyelination and regeneration after nerve injury in adulthood. *J. Neurosci.* **31**, 3225-3233.

Fu, A. K., Cheung, W. M., Ip, F. C. and Ip, N. Y. (1999). Identification of genes induced by neuregulin in cultured myotubes. *Mol. Cell Neurosci.* **14**, 241-253.

Fu, A. K., Ip, F. C., Fu, W. Y., Cheung, J., Wang, J. H., Yung, W. H. and Ip, N. Y. (2005). Aberrant motor axon projection, acetylcholine receptor clustering, and neurotransmission in cyclin-dependent kinase 5 null mice. *Proc. Natl. Acad. Sci. USA* **102**, 15224-15230.

Fuhrer, C., Sugiyama, J. E., Taylor, R. G. and Hall, Z. W. (1997). Association of muscle-specific kinase MuSK with the acetylcholine receptor in mammalian muscle. *EMBO J.* **16**, 4951-4960.

Gautam, M., Noakes, P. G., Mudd, J., Nichol, M., Chu, G. C., Sanes, J. R. and Merlie, J. P. (1995). Failure of postsynaptic specialization to develop at neuromuscular junctions of rapsyn-deficient mice. *Nature* **377**, 232-236.

Gautam, M., Noakes, P. G., Moscoso, L., Rupp, F., Scheller, R. H., Merlie, J. P. and Sanes, J. R. (1996). Defective neuromuscular synaptogenesis in agrin-deficient mutant mice. *Cell* **85**, 525-535.

Gee, S. H., Montanaro, F., Lindenbaum, M. H. and Carbonetto, S. (1994). Dystroglycan-alpha, a dystrophin-associated glycoprotein, is a functional agrin receptor. *Cell* **77**, 675-686.

Ghazanfari, N., Fernandez, K. J., Murata, Y., Morsch, M., Ngo, S. T., Reddel, S. W., Noakes, P. G. and Phillips, W. D. (2010). Muscle Specific Kinase: Organiser of synaptic membrane domains. *Int. J. Biochem. Cell Biol.* **43**, 295-298.

Glass, D. J., Bowen, D. C., Stitt, T. N., Radziejewski, C., Bruno, J., Ryan, T. E., Gies, D. R., Shah, S., Mattsson, K., Burden, S. J. et al. (1996). Agrin acts via a MuSK receptor complex. *Cell* **85**, 513-523.

Han, H., Noakes, P. G. and Phillips, W. D. (1999). Overexpression of rapsyn inhibits agrin-induced acetylcholine receptor clustering in muscle cells. *J. Neurocytol.* **28**, 763-775.

Herbst, R. and Burden, S. J. (2000). The juxtamembrane region of MuSK has a critical role in agrin-mediated signaling. *EMBO J.* **19**, 67-77.

Hoch, W. (1999). Formation of the neuromuscular junction. Agrin and its unusual receptors. *Eur. J. Biochem.* **265**, 1-10.

Hoch, W., Ferns, M., Campanelli, J. T., Hall, Z. W. and Scheller, R. H. (1993). Developmental regulation of highly active alternatively spliced forms of agrin. *Neuron* **11**, 479-490.

Ip, F. C., Glass, D. G., Gies, D. R., Cheung, J., Lai, K. O., Fu, A. K., Yancopoulos, G. D. and Ip, N. Y. (2000). Cloning and characterization of muscle-specific kinase in chicken. *Mol. Cell. Neurosci.* **16**, 661-673.

Jaworski, A. and Burden, S. J. (2006). Neuromuscular synapse formation in mice lacking motor neuron- and skeletal muscle-derived Neuregulin-1. *J. Neurosci.* **26**, 655-661.

Jaworski, A., Smith, C. L. and Burden, S. J. (2007). GA-binding protein is dispensable for neuromuscular synapse formation and synapse-specific gene expression. *Mol. Cell. Biol.* **27**, 5040-5046.

Jo, S. A., Zhu, X., Marchionni, M. A. and Burden, S. J. (1995). Neuregulins are concentrated at nerve-muscle synapses and activate ACh-receptor gene expression. *Nature* **373**, 158-161.

Kim, N., Stiegler, A. L., Cameron, T. O., Hallock, P. T., Gomez, A. M., Huang, J. H., Hubbard, S. R., Dustin, M. L. and Burden, S. J. (2008). Lrp4 is a receptor for Agrin and forms a complex with MuSK. *Cell* **135**, 334-342.

Lacazette, E., Le Calvez, S., Gajendran, N. and Brenner, H. R. (2003). A novel pathway for MuSK to induce key genes in neuromuscular synapse formation. *J. Cell Biol.* **161**, 727-736.

Leu, M., Bellmunt, E., Schwander, M., Farinas, I., Brenner, H. R. and Muller, U. (2003). Erbb2 regulates neuromuscular synapse formation and is essential for muscle spindle development. *Development* **130**, 2291-2301.

Li, Q. and Loeb, J. A. (2001). Neuregulin-heparan-sulfate proteoglycan interactions produce sustained erbB receptor activation required for the induction of acetylcholine receptors in muscle. *J. Biol. Chem.* **276**, 38068-38075.

Lin, S., Maj, M., Bezakova, G., Magyar, J. P., Brenner, H. R. and Ruegg, M. A. (2008). Muscle-wide secretion of a miniaturized form of neural agrin rescues focal neuromuscular innervation in agrin mutant mice. *Proc. Natl. Acad. Sci. USA* **105**, 11406-11411.

Lin, W., Dominguez, B., Yang, J., Aryal, P., Brandon, E. P., Gage, F. H. and Lee, K. F. (2005). Neurotransmitter acetylcholine negatively regulates neuromuscular synapse formation by a cdk5-dependent mechanism. *Neuron* **46**, 569-579.

Loeb, J. A. (2003). Neuregulin: an activity-dependent synaptic modulator at the neuromuscular junction. *J. Neurocytol.* **32**, 649-664.

Loeb, J. A., Khurana, T. S., Robbins, J. T., Yee, A. G. and Fischbach, G. D. (1999). Expression patterns of transmembrane and released forms of neuregulin during spinal cord and neuromuscular synapse development. *Development* **126**, 781-791.

Lupa, M. T. and Hall, Z. W. (1989). Progressive restriction of synaptic vesicle protein to the nerve terminal during development of the neuromuscular junction. *J. Neurosci.* **9**, 3937-3945.

Madhavan, R. and Peng, H. B. (2005). Molecular regulation of postsynaptic differentiation at the neuromuscular junction. *IUBMB Life* **57**, 719-730.

Madhavan, R., Zhao, X. T., Ruegg, M. A. and Peng, H. B. (2005). Tyrosine phosphatase regulation of MuSK-dependent acetylcholine receptor clustering. *Mol. Cell. Neurosci.* **28**, 403-416.

Magill-Solc, C. and McMahan, U. J. (1988). Motor neurons contain agrin-like molecules. *J. Cell Biol.* **107**, 1825-1833.

Magill-Solc, C. and McMahan, U. J. (1990). Synthesis and transport of agrin-like molecules in motor neurons. *J. Exp. Biol.* **153**, 1-10.

Martinou, J. C., Falls, D. L., Fischbach, G. D. and Merlie, J. P. (1991). Acetylcholine receptor-inducing activity stimulates expression of the epsilon-subunit gene of the muscle acetylcholine receptor. *Proc. Natl. Acad. Sci. USA* **88**, 7669-7673.

McMahan, U. J. (1990). The agrin hypothesis. *Cold Spring Harb. Symp. Quant. Biol.* **55**, 407-418.

Meijer, L., Borgne, A., Mulner, O., Chong, J. P., Blow, J. J., Inagaki, N., Inagaki, M., Delcros, J. G. and Moulinoux, J. P. (1997). Biochemical and cellular effects of roscovitine, a potent and selective inhibitor of the cyclin-dependent kinases cdc2, cdk2 and cdk5. *Eur. J. Biochem.* **243**, 527-536.

Merlie, J. P. and Sanes, J. R. (1985). Concentration of acetylcholine receptor mRNA in synaptic regions of adult muscle fibres. *Nature* **317**, 66-68.

Meyer, D., Yamaai, T., Garratt, A., Riethmacher-Sonnenberg, E., Kane, D., Theill, L. E. and Birchmeier, C. (1997). Isoform-specific expression and function of neuregulin. *Development* **124**, 3575-3586.

Mittaud, P., Camilleri, A. A., Willmann, R., Erb-Vogtli, S., Burden, S. J. and Fuhrer, C. (2004). A single pulse of agrin triggers a pathway that acts to cluster acetylcholine receptors. *Mol. Cell. Biol.* **24**, 7841-7854.

Moscoso, L. M., Chu, G. C., Gautam, M., Noakes, P. G., Merlie, J. P. and Sanes, J. R. (1995). Synapse-associated expression of an acetylcholine receptor-inducing protein, ARIA/heregulin, and its putative receptors, ErbB2 and ErbB3, in developing mammalian muscle. *Dev. Biol.* **172**, 158-169.

Ngo, S. T., Balke, C., Phillips, W. D. and Noakes, P. G. (2004). Neuregulin potentiates agrin-induced acetylcholine receptor clustering in myotubes. *Neuroreport* **15**, 2501-2505.

Ngo, S. T., Noakes, P. G. and Phillips, W. D. (2007). Neural agrin: A synaptic stabiliser. *Int. J. Biochem. Cell Biol.* **39**, 863-867.

Noakes, P. G., Phillips, W. D., Hanley, T. A., Sanes, J. R. and Merlie, J. P. (1993). 43K protein and acetylcholine receptors colocalize during the initial stages of neuromuscular synapse formation in vivo. *Dev. Biol.* **155**, 275-280.

Noakes, P. G., Chin, D., Kim, S. S., Liang, S. and Phillips, W. D. (1999). Expression and localization of dynamin and syntaxin during neural development and neuromuscular synapse formation. *J. Comp. Neurol.* **410**, 531-540.

O'Leary, D. A., Noakes, P. G., Lavidis, N. A., Kola, I., Hertzog, P. J. and Ristevski, S. (2007). Targeting of the ETS factor GABPalpha disrupts neuromuscular junction synaptic function. *Mol. Cell. Biol.* **27**, 3470-3480.

Ponomareva, O. N., Ma, H., Vock, V. M., Ellerton, E. L., Moody, S. E., Dakour, R., Chodosh, L. A. and Rimer, M. (2006). Defective neuromuscular synaptogenesis in mice expressing constitutively active ErbB2 in skeletal muscle fibers. *Mol. Cell. Neurosci.* **31**, 334-345.

Qian, Y. K., Chan, A. W., Madhavan, R. and Peng, H. B. (2008). The function of Shp2 tyrosine phosphatase in the dispersal of acetylcholine receptor clusters. *BMC Neurosci.* **9**, 70.

Reist, N. E., Werle, M. J. and McMahan, U. J. (1992). Agrin released by motor neurons induces the aggregation of acetylcholine receptors at neuromuscular junctions. *Neuron* **8**, 865-868.

Rupp, F., Hoch, W., Campanelli, J. T., Kreiner, T. and Scheller, R. H. (1992). Agrin and the organization of the neuromuscular junction. *Curr. Opin. Neurobiol.* **2**, 88-93.

Sanes, J. R. and Lichtman, J. W. (1999). Development of the vertebrate neuromuscular junction. *Annu. Rev. Neurosci.* **22**, 389-442.

Sanes, J. R. and Lichtman, J. W. (2001). Induction, assembly, maturation and maintenance of a postsynaptic apparatus. *Nat. Rev. Neurosci.* **2**, 791-805.

Slevin, J. C., Byers, L., Gertsenstein, M., Qu, D., Mu, J., Sunn, N., Kingdom, J. C., Rossant, J. and Adamson, S. L. (2006). High resolution ultrasound-guided microinjection for interventional studies of early embryonic and placental development in vivo in mice. *BMC Dev. Biol.* **6**, 10.

Smith, C. L., Mittaud, P., Prescott, E. D., Fuhrer, C. and Burden, S. J. (2001). Src, Fyn, and Yes are not required for neuromuscular synapse formation but are necessary for stabilization of agrin-induced clusters of acetylcholine receptors. *J. Neurosci.* **21**, 3151-3160.

Strochlic, L., Cartaud, A. and Cartaud, J. (2005). The synaptic muscle-specific kinase (MuSK) complex: New partners, new functions. *BioEssays* **27**, 1129-1135.

Tanowitz, M., Si, J., Yu, D. H., Feng, G. S. and Mei, L. (1999). Regulation of neuregulin-mediated acetylcholine receptor synthesis by protein tyrosine phosphatase SHP2. *J. Neurosci.* **19**, 9426-9435.

Trachtenberg, J. T. and Thompson, W. J. (1997). Nerve terminal withdrawal from rat neuromuscular junctions induced by neuregulin and Schwann cells. *J. Neurosci.* **17**, 6243-6255.

Trinidad, J. C. and Cohen, J. B. (2004). Neuregulin inhibits acetylcholine receptor aggregation in myotubes. *J. Biol. Chem.* **279**, 31622-31628.

Trinidad, J. C., Fischbach, G. D. and Cohen, J. B. (2000). The Agrin/MuSK signaling pathway is spatially segregated from the neuregulin/ErbB receptor signaling pathway at the neuromuscular junction. *J. Neurosci.* **20**, 8762-8770.

Tsujinaka, T., Kajiwara, Y., Kambayashi, J., Sakon, M., Higuchi, N., Tanaka, T. and Mori, T. (1988). Synthesis of a new cell penetrating calpain inhibitor (calpeptin). *Biochem. Biophys. Res. Commun.* **153**, 1201-1208.

Valdez, G., Tapia, J. C., Kang, H., Clemenson, G. D., Jr, Gage, F. H., Lichtman, J. W. and Sanes, J. R. (2010). Attenuation of age-related changes in mouse neuromuscular synapses by caloric restriction and exercise. *Proc. Natl. Acad. Sci. USA* **107**, 14863-14868.

Valenzuela, D. M., Stitt, T. N., DiStefano, P. S., Rojas, E., Mattsson, K., Compton, D. L., Nunez, L., Park, J. S., Stark, J. L., Gies, D. R. et al. (1995). Receptor tyrosine kinase specific for the skeletal muscle lineage: expresion in embryonic muscle, at the neuromuscular junction, and after injury. *Neuron* **15**, 573-584.

Wilson, M. H. and Deschenes, M. R. (2005). The neuromuscular junction: anatomical features and adaptations to various forms of increased, or decreased neuromuscular activity. *Int. J. Neurosci.* **115**, 803-828.

Wu, H., Xiong, W. C. and Mei, L. (2010). To build a synapse: signaling pathways in neuromuscular junction assembly. *Development* **137**, 1017-1033.

Zhang, B., Luo, S., Wang, Q., Suzuki, T., Xiong, W. C. and Mei, L. (2008). LRP4 serves as a coreceptor of agrin. *Neuron* **60**, 285-297.

Zhao, X. T., Qian, Y. K., Chan, A. W., Madhavan, R. and Peng, H. B. (2007). Regulation of ACh receptor clustering by the tyrosine phosphatase Shp2. *Dev. Neurobiol.* **67**, 1789-1801.

Zhu, X., Lai, C., Thomas, S. and Burden, S. J. (1995). Neuregulin receptors, erbB3 and erbB4, are localized at neuromuscular synapses. *EMBO J.* **14**, 5842-5848.

Journal of Cell Science